

# Transformation Processes in the Oder Lagoon as seen from a Model Perspective

Thomas Neumann<sup>1</sup>, Gerald Schernewski<sup>1</sup>, and René Friedland<sup>1</sup>

<sup>1</sup>Leibniz Institute for Baltic Sea Research Warnemünde, 18119 Warnemünde, Germany

**Correspondence:** Thomas Neumann (thomas.neumann@io-warnemuende.de)

**Abstract.** The Oder/Szczecin Lagoon is one of the largest Baltic Sea lagoons and is subject to very high nutrient loads from the Oder/Odra River. For our study, we employ a modified, high-resolution 3D ecosystem model specifically adapted for this shallow lagoon. The model demonstrates stable and reliable performance over 25 years of simulation (1995 – 2019), enabling a detailed assessment of lagoon processes under various scenarios. Our model simulations indicate that changes in riverine 5 nutrient inputs have an immediate impact on the lagoon’s water quality, affecting parameters such as phytoplankton biomass and water transparency.

Hypoxia is a prevalent phenomenon, affecting most parts of the lagoon which promotes internal eutrophication. On average, the lagoon retains 12% (253 t/year) of the phosphorus and 40% (17,278 t/year) of the nitrogen riverine inputs. The primary sink process for phosphorus is sediment burial, and for nitrogen, it is denitrification. Nitrogen retention decreases with increasing 10 riverine loads, dropping to around 30% during years with exceptionally high inputs. **In contrast, phosphorus retention is independent on loads.** The nutrient retention capacity of the lagoon has significant implications for Baltic Sea eutrophication but is not currently accounted for in major policies and Baltic Sea models.

Although recent nutrient loads from the Oder River comply with policy targets, such as the Baltic Sea Action Plan’s maximum allowable inputs and Germany’s river targets, these levels are insufficient to improve the lagoon’s ecological state sufficiently. The Oder Lagoon remains in a highly eutrophic condition, making the achievement of a good ecological status unlikely 15 under the current management targets.

## 1 Introduction

Marine ecosystems around the world suffer from increasing oxygen deficiencies (Diaz and Rosenberg, 2008). Especially coastal zones are affected by permanent or seasonal low oxic conditions (Fennel and Testa, 2019; Conley et al., 2011; Carstensen et al., 20 2014). The drivers of deoxygenation are land and airborne nutrient depositions and increased temperature (Kabel et al., 2012; Börgel et al., 2023). Coastal features such as lagoons and bays can significantly reduce terrestrial nutrient loads. This is due to their long residence time and shallow waters. Shallow waters facilitate a close interaction between sedimentary processes and those in the euphotic zone, thereby speeding up biogeochemical cycles (e.g. Asmala et al., 2017).

The Baltic Sea includes a diverse array of coastal waters, bays, lagoons, and estuaries, each with unique features and behaviors. These waters host specialized flora and fauna and act as transformers and retention units for external nutrient loads. 25

Asmala et al. (2017) classified Baltic Sea coastal ecosystems into different categories: lagoons, estuaries, embayments, open coast, and archipelago. For nitrogen removal (denitrification), lagoons have the highest rate, followed by estuaries. Within the lagoons, the Oder Lagoon is the region with the highest denitrification rate. In the case of phosphorus retention (burial in their study), archipelagos show the highest potential, which is driven by the import of phosphorus from the open sea.

30 Systems with prolonged water residence times and high nutrient loads are particularly important for Baltic Sea pollution. Only a few coastal waters can significantly alter nutrient loads transported from rivers to the Baltic Sea. Notable examples include the Curonian and Vistula Lagoons, the Gulf of Riga, coastal waters near St. Petersburg, and some Scandinavian estuaries. Among these, the Oder Lagoon is likely the most critical system in terms of quantitative nutrient retention and transformation (Vybernaite-Lubiene et al., 2022; Müller-Karulis and Aigars, 2011; Almroth-Rosell et al., 2016; Edman et al., 2018; Kuliński et al., 2022).

35 Asmala et al. (2017) studied the coastal filter for the entire Baltic Sea by observations of denitrification and sediment cores. Their results suggest a removal of 16% nitrogen and 53% of phosphorus from the land based loads. Swedish coastal waters exhibit a relatively high nutrient retention capability. Edman et al. (2018) reported a mean phosphorus retention of 69% and a mean nitrogen retention of 53% estimated from model simulations. These high values, particularly for phosphorus, are due to 40 the oxic water conditions, which favor the trapping of phosphorus in the sediment.

45 The shallow Oder Lagoon, located at the German/Polish border in the southern Baltic Sea, is one of the largest lagoons in Europe. With an average water discharge of about 500 m<sup>3</sup>/s and a drainage area of about 120,000 km<sup>2</sup>, the Oder River is one of the most important rivers in the Baltic Sea catchment. Due to similarities with other lagoons, it can be expected that insights into retention and transformation processes can be related to driving factors, and simplified relationships can be transferred to other systems. By studying the most important coastal water systems in detail, load calculations to the Baltic Sea can be systematically improved, enhancing regional ecosystem state and water quality assessments.

50 The European Water Framework Directive (WFD) is the primary legislation aimed at achieving good ecological status in European coastal and transitional waters. Under the WFD, these systems are classified as distinct water bodies, which undergo regular monitoring. Consequently, long-term data on Baltic coastal waters are available, with some records dating back to the 1970s for most countries. However, these data are typically collected fortnightly from a single station intended to represent the entire system. While this is adequate for assessing averaged overall states and long-term changes, the limited spatial and temporal resolution hinders the analysis and understanding of major processes within these systems and their annual dynamics. Increasing the frequency of sampling and the number of locations would raise costs beyond feasible levels. Therefore, combining 3D ecosystem models with field data is necessary.

55 Additionally, the Baltic Sea Action Plan (BSAP) (HELCOM, 2021a) establishes the maximum allowable inputs (MAI) for nitrogen and phosphorus required to achieve a good environmental status (Schernewski et al., 2015) in the Baltic Sea. These inputs describe loads to the open Baltic Sea and do not consider possible modifications within the coastal filter, particularly lagoons where large rivers enter.

60 Recent high-resolution 3D ecosystem models of the Baltic Sea, such as presented by Piehl et al. (2023), effectively and sufficiently describe processes for practical purposes like policy implementation and state assessments. However, these models

fall short in semi-enclosed, enclosed, and several transitional waters due to inadequate spatial resolution. Currently, neither data nor models adequately account for retention and transformation processes in these systems, leading to overestimated nutrient loads to the Baltic Sea.

These deficiencies have been compensated for, for example, by making assumptions about the bioavailability of riverine nutrients. Eilola et al. (2011) state that the three considered models differ in their assumptions of bioavailability and discuss uncertainties in these assumptions. Ruvalcaba Baroni et al. (2024) use reduction factors for nutrient inputs in their model study because nutrient removal for different coastal types is poorly quantified. They also argue that river-specific organic matter retention factors in coastal waters would improve the [input representation](#) of organic matter [from rivers](#)[inputs from rivers in models](#).

70 The quantitatively unknown nutrient retention in coastal waters could potentially result in inaccurate policy settings, such as maximum allowable inputs or water quality thresholds and targets. Our objectives are to:

- (a) set up a [spatially high resolved high-spatial-resolution](#) ecosystem model for the Oder Lagoon;
- (b) apply and validate the 3D ecosystem model in the Oder Lagoon using long-term data;
- (c) quantify the retention of nitrogen and phosphorus and their inter-annual variability in the lagoon;
- 75 (d) analyze the driving parameters; and
- (e) assess the consequences for policy implementation, namely water quality thresholds, acceptable riverine loads, as well as lagoon and Baltic Sea management.

## 2 Model Setup

We employ a numerical modeling technique to evaluate ecosystem dynamics in the Oder Lagoon. The model integrates both 80 biogeochemical and circulation components. The hydrodynamic core utilizes the Modular Ocean Model (MOM5.1, Griffies, 2004), dynamically coupled with a sea ice model (Winton, 2000). The sea ice component implements:

- (a) A three-layer vertical thermodynamic scheme
- (b) Multiple ice thickness categories with dynamic redistribution
- (c) Category transition mechanisms responding to thermodynamic and mechanical forcing
- 85 (d) Full ice dynamics incorporating internal stresses via an elastic-viscous-plastic rheology

This coupled configuration enables comprehensive simulation of both physical transport processes and biogeochemical transformations in the lagoon system.

The biogeochemical part of the [mode model is](#) based on ERGOM version 1.2 (Leibniz Institute for Baltic Sea Research, 2015). A detailed explanation and validation of the model can be found in (Neumann et al., 2022). For this study, the model 90 was specifically set up for the Oder Lagoon area within the Baltic Sea. Figure 1 illustrates the bathymetry of the model. A notable aspect is the navigation channel, which has a depth of 10 m. Modifications to the Świna River began in 1721, and in 1880, a shortened and deepened artificial channel was completed. Subsequent dredging projects increased the depth to 9.6 meters in 1939 and to 10.5 meters in 1984 across the entire lagoon. Most recently, between 2018 and 2023, the entire waterway

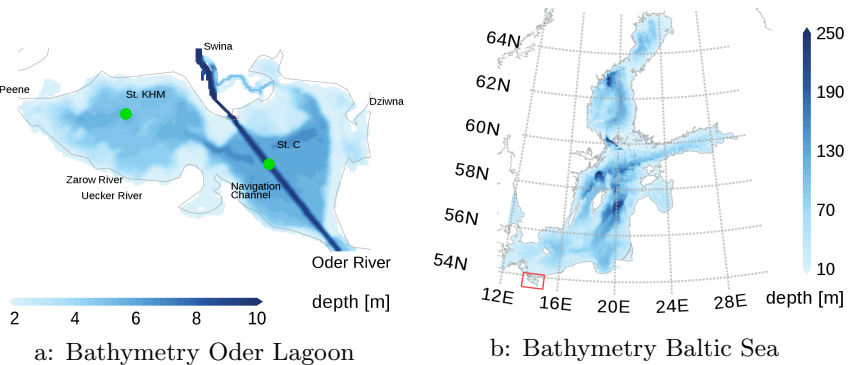


**Figure 1.** Bathymetric map of the Oder Lagoon model (a). The green dots indicate two stations used for validation. Peene, Świna, and Dziwna mark the locations of the open boundary conditions, and Oder, Uecker, and Zarow Rivers represent the river mouths. The red rectangle in (b) shows the location of the Oder Lagoon within the Baltic Sea. The map was created using the software package GrADS 2.1.1.b0 (<http://cola.gmu.edu/grads/>, last access: 28 November 2024), using published bathymetry data (Seifert et al., 2008).

through the Oder Lagoon was deepened to 12.5 meters (Schernewski et al., 2025a). Beyond the channel, the lagoon remains relatively shallow with depths predominantly under 5 m. The horizontal grid resolution is 150 m (altogether 330x191 grid points). Vertically, the model is divided into 28 layers, starting with a layer thickness of 25 cm at the top and 50 cm at the bottom. Three open boundary conditions (OBC), Peene, Świna, and Dziwna in Fig. 1, link the model to the Baltic Sea. Data from a coarser Baltic Sea model with a 2 km resolution (Piehl et al., 2023) are applied at the OBC locations. The Oder River enters into the lagoon from the southern edge.

The ERGOM model describes cycles of nitrogen, phosphorus, carbon, oxygen, and partially sulfur. Primary production is driven by photosynthetically active radiation, facilitated by four functional groups of phytoplankton (large cells, small cells, limnic phytoplankton, and cyanobacteria). The optical sub-model estimates the light [climate field](#) based on chlorophyll and CDOM (Colored Dissolved Organic Matter) concentrations (Neumann et al., 2021). Dead organic matter accumulates in the detritus state variable. Bulk zooplankton grazes on phytoplankton and represents the highest trophic level considered in the model. Particulate organic matter (POC: phytoplankton, detritus, and other POC species) have the capability to sink into the water column and accumulate within a sediment layer.

The sediment module parameterizes key early diagenetic processes, including coupled nitrification-denitrification, organic matter remineralization, iron-phosphate complex formation/dissolution dynamics, and permanent burial. These processes are vertically integrated and represented through a two-dimensional model variable. Under oxic conditions at the sediment-water interface, phosphate binds to ferric iron  $\text{Fe}^{3+}$  to form particulate complexes. Hydrodynamic erosion may subsequently resuspend these iron-bound phosphate particles, facilitating their transport via bottom currents to depositional zones. Conversely, under anoxic conditions, iron oxides undergo reductive dissolution, releasing phosphate into the overlying water column as

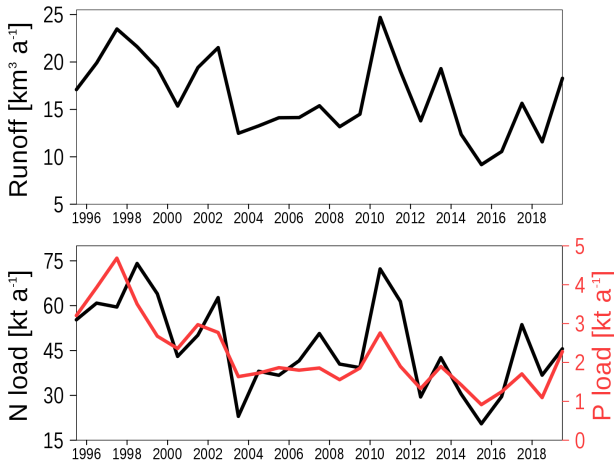


**Figure 2.** Riverine forcing of the model. Upper panel: Annual mean runoff. Lower panel: Annual mean loads for nitrogen (black) and phosphorus (red).

dissolved inorganic phosphorus, following established redox-sensitive phosphorus cycling mechanisms (Neumann and Schernewski, 2008).

115 Detritus undergoes mineralization into dissolved inorganic nitrogen and phosphorus both in the water column and in the sediment. The mineralization process is influenced by water temperature and oxygen concentration. Oxygen is produced through primary production and consumed by processes such as metabolism and mineralization. Furthermore, phytoplankton excrete extracellular dissolved organic matter with non-Redfield stoichiometry, resulting in non-Redfield carbon uptake, while maintaining canonical Redfield ratios within their cellular composition.

120 In addition to the model proposed by Neumann et al. (2022), we have introduced a fourth phytoplankton group (limnic phytoplankton). This new group is specifically designed for low salinity and turbid coastal waters, realizing growth limitations due to high salinity levels as well as increased light sensitivity.

All organic particles (phytoplankton, detritus, etc.) are counted in nitrogen units. To compare the model phytoplankton with chlorophyll observations, we sum up all phytoplankton groups and multiply them by a constant chlorophyll-to-carbon ratio.

125 At the open boundaries, the model is forced by data from a coarse grained model as noted above. Meteorological forcing data are from the coastDat-3 dataset (Geyer and Rockel, 2013). It is the same data set forcing the coarse grained model. Nutrient loads and runoff into the lagoon from rivers Oder, Ücker, and Zarow were provided by Polish and German national agencies (see *code and data availability*). The riverine forcing is shown in Fig. 2. Loads are correlated with runoff, that is, the interannual runoff variability predominantly controls the load's variability. A minor fraction of the total nutrient loads enters the lagoon 130 through the limnic phytoplankton state variable, which ensures seed concentrations near the river mouth. Riverine CDOM concentrations are prescribed using a monthly climatology, as described in detail by Neumann et al. (2021). Atmospheric deposition of nitrogen and phosphorus is realized as a boundary condition (air-sea fluxes) based on data provided by HELCOM

assessments (e.g. HELCOM) which are originated from EMEP (<https://www.eea.europa.eu/data-and-maps/data/external/emepe-n-atmospheric-deposition>).

135 We start the model simulations in 1995 initialized with data from Piehl et al. (2023) and run it until 2019. For analysis of the simulations, we diagnosed two-day means of all relevant state variables, processes, and transports. For the analysis of our results, we derived diagnostic variables from the model state variables:

- (a) Secchi depth as a function of water constituents: Neumann et al. (2015).
- (b) Chlorophyll: The sum of phytoplankton model variables multiplied with a constant chlorophyll to carbon mass ratio of 40 (e.g., Neumann et al., 2015).

The observed statistical relationships were evaluated using Spearman rank correlation tests, with significance assessed via p-values. The null hypothesis ( $H_0$ ) posits no correlation between the examined variables. If the calculated p-value falls below the conventional significance threshold (typically  $\alpha = 0.05$ ), we reject the null hypothesis, thereby providing statistical evidence for a significant relationship between the variables.

## 145 3 Results

First, we will assess the model's performance, followed by presenting the results from its runs.

### 3.1 Model Skill Evaluation

The model reasonably Appendix A presents an expanded model performance analysis. We evaluate time series and climatology of hydrodynamic (temperature, salinity, stratification, and mass transport), and biogeochemical (nutrients, chlorophyll-a, 150 and bottom oxygen) parameters.

The model reasonably reproduces the climatology as well as the interannual variability of nutrients, temperature, and salinity at stations KHM and C (for station locations, see Fig. 1). For bottom oxygen (Figs. A1 and A2), the model predicts lower values than in the observations. Reasons are that (i) measurements are not as close to the bottom as the model data, (ii) the measurement platform (vessel) itself disturbs the stratification, and (iii) at station C commercial ship traffic induces strong 155 vertical mixing which is not part of the model.

The mass transport through the Dziwna channel (for location, see Fig. 1) is elevated compared to known values (Fig. A6). The reason is the truncated Dziwna channel in the model reducing the hydraulic resistance and facilitating an enhanced discharge at the expense of a lower discharge through the Swina channel.

The stratification of the water column at station KHM (for location, see Fig. 1) compares well with observed stratification (Fig. A8). Stratification establishes as events, such as those in summer, while during winter the water is well mixed. Stratification results in oxygen deficiencies, which yield phosphate liberation from the sediment. This process is not directly observed but is indirectly indicated by elevated phosphorus concentrations in summer (Fig. A7).

An extended analysis of the model performance is provided in Appendix A.

Our evaluation confirms that the model reasonably represents the Oder Lagoon ecosystem's key dynamics, establishing it as a reliable tool for experimental analysis and system property investigation.

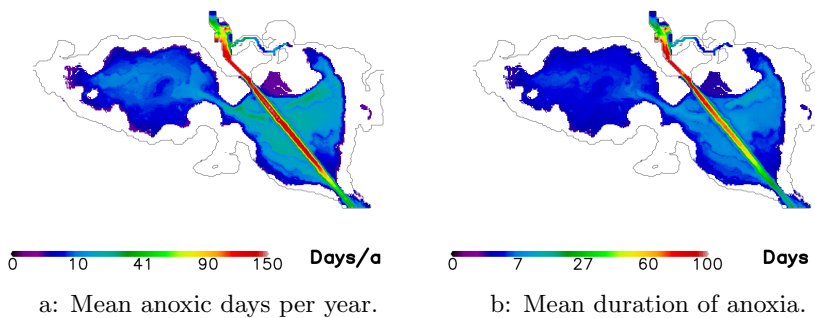


**Figure 3.** The mean number of days of anoxia per year (a) and the mean duration of anoxia (b). Numbers are calculated as mean over the simulation period 1995–2019. The map was created using the software package GrADS 2.1.1.b0 (<http://cola.gmu.edu/grads/>, last access: 28 November 2024), using published bathymetry data (Seifert et al., 2008).

### 3.2 Oxygen dynamics

Due to the shallow bathymetry, the water column is well-mixed during winter. However, in summer, stratification may occur, and elevated temperatures accelerate metabolic processes, potentially leading to anoxic conditions in bottom waters. Figure 3a illustrates the total number of oxygen-depleted (zero oxygen concentration) days, while Fig. 3b shows the average duration of 170 these anoxic events. A notable region of anoxia is found in the navigation channel, which is 10 meters deep – approximately 5 meters deeper than the surrounding area. This deeper channel acts as a sediment trap, increasing oxygen demand for sediment respiration. Additionally, ventilation from the surface occurs less frequently here compared to other regions due to the greater water depth. Aside from the navigation channel, the eastern part of the lagoon is more affected by anoxia than the western part. This is likely due to the high nutrient loads from the Oder River entering the eastern lagoon.

### 175 3.3 Filter function

Lagoons play an important ecological role, particularly through their filtering function, which is crucial for nutrient management. Biogeochemical processes within the lagoon help retain or remove nutrients from the system. Consequently, the amount of nutrients entering the open sea is reduced compared to the amount entering the lagoon.

In this section, we relate nutrient sources to their sinks to determine the proportion of nutrient loads removed within the 180 lagoon. Additionally, the retention capacity of the Oder Lagoon may be sensitive to variations in nutrient loads. To evaluate this sensitivity, we performed an additional simulation with a 50% reduction in nutrient input, allowing us to assess how such changes influence the lagoon's filtering capacity. The results are presented in Fig. 4.

Sources of nitrogen and phosphorus primarily include riverine loads and atmospheric deposition, with riverine loads being the dominant contributor. An additional source of nitrogen is nitrogen fixation by cyanobacteria. Phosphorus has a single sink 185 in the system – burial in the sediment. In contrast, nitrogen has an additional sink through denitrification, occurring both in

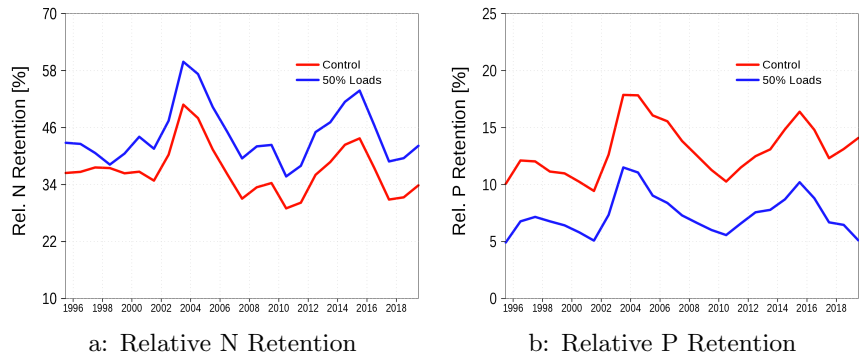


**Figure 4.** The relative retention capacity of the Oder lagoon for nitrogen (a) and phosphorus (b). The blue line is the sensitivity simulation with halved loads.

the water column and the sediment. These factors help explain the contrasting responses of phosphorus and nitrogen retention capacities to changes in nutrient loads. For phosphorus, reduced loads lead to a decrease in primary production, which results in less organic matter reaching the sediment for burial. For nitrogen, burial also decreases; however, denitrification in the sediment increases because of the greater availability of oxygen.

190 In the next step, we are testing whether there exists a robust relationship between the retention capacity and the loads for nitrogen and phosphorus. For this purpose, we combined data from the reference run and the run with halved loads to increase the range of loads and consider the annual means. Figure 5a,c shows the absolute numbers of loads (source) into the system and the retention (sink). The retention increases with the loads, but is this retention at the same rate for all load realizations? Figure 4 suggests that the rate changes with the loads. A detailed dependence of the retention rate on loads is given in Fig. 5b,d. In the 195 case of nitrogen, the retention rate significantly decreases with increasing loads ( $p = 0$ ). In contrast, a significant relationship between the retention rate and phosphorus loads does not exist, as Fig. 4b suggests. A t-test for the regression coefficient confirms the visual indication. Consequently, Spearman rank correlation test yields a non-significant regression coefficient ( $p = 0.68$ ). This result fails to reject the null hypothesis of no correlation, thereby indicating that the apparent differences in the difference seen in Fig. 4b is statistically not significant are not statistically significant at conventional confidence levels.

200 Our analysis reveals a further relationship between nitrogen and phosphorus retention efficiency and the lagoon's water residence time (Fig. 6). The relationship for phosphorus is less pronounced but statistically robust ( $p(N) = 0.0004$ ,  $p(P) = 0.0017$ ). While a similar correlation exists for phosphorus, it appears less pronounced (Fig. 6). In general, we can state that the longer water remains in the lagoon, the higher the relative retention of nutrients in the lagoon.

205 In summary, the nitrogen retention capacity is stronger than that of phosphorus, primarily due to denitrification. Approximately The mean of the annual retention over the 25 years simulation period is approximately 40% for nitrogen and 12% of phosphorus are retained in the lagoon. Reduced nutrient loads to the lagoon increase the nitrogen retention capacity, while the phosphorus retention capacity remains largely independent of load variations. Nitrogen retention capacity increases with reduced lagoon nutrient loads, while

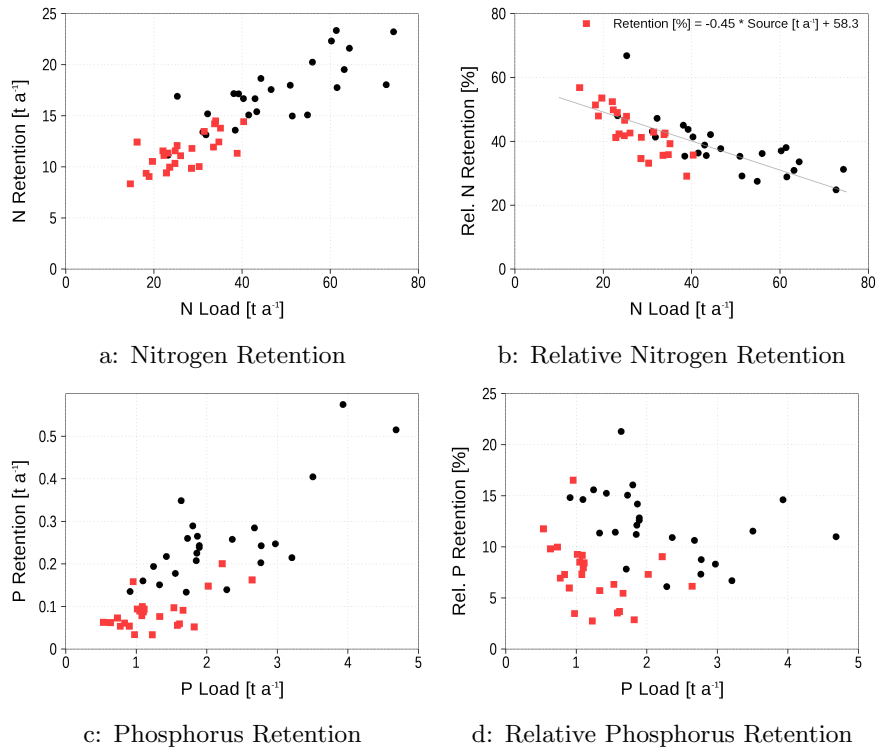


**Figure 5.** Annual means of nitrogen and phosphorus retention (a, c) and relative retention (b, d) in dependence on the loads. Red squares are from the 50% reduced loads experiment, black dots from the control run.

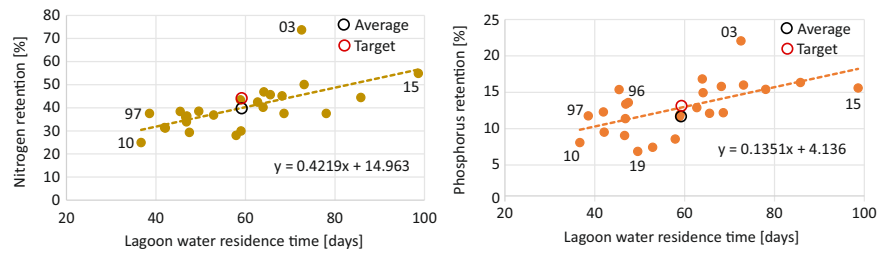


**Figure 6.** Relationship between average annual water residence time and the nitrogen and phosphorus retention in the Oder lagoon. Residence time has been estimated following Vollenweider (1976); Monsen et al. (2002) by lagoon's volume over runoff. Targets are the allowable loads defined by the BSAP. **Both correlations are highly significant ( $p < 0.002$ ), indicating strong non-random associations between variables.**

phosphorus retention remains largely load-independent, statistically confirmed by analysis of Fig. 5d data. It is important

**Table 1.** Sinks and sources (loads, N-fixation) of nitrogen and phosphorus in the Oder Lagoon in kt/a. Shown are mean values for the simulation period.

	N [kt/a]	P [kt/a]
Loads	46.5	2.2
N-Fixation	1.3	
Denitrification Sed.	13.7	
Denitrification Pelag.	1.8	
Burial	1.8	0.25

to note that this statement is valid only for the load range applied in the simulations. Mean numbers of sources and sinks are

210 summarized in Tab. 1.

### 3.4 Annual discharge, nutrient loads and water quality targets

The Oder River contributes about 98% of the direct water discharge to the lagoon, while the remaining 2% is contributed by the Zarow and Uecker rivers. The total water discharge into the lagoon, along with the loads of nitrogen (N) and phosphorus (P), exhibits similar temporal behavior (Fig. 7a). Between 1995 and 2019, the average water discharge was  $518 \text{ m}^3/\text{s}$ , with

215 average annual total loads of 46,266 t N and 2,198 t P to the lagoon. Between 1995 and 1999, the average water discharge was  $643 \text{ m}^3/\text{s}$ , which is higher than the average over the 25-year model simulation period. Consequently, the annual N loads

(62,534 t N) and P loads (3,600 t P) were also higher. In contrast, during the recent years between 2015 and 2019, the average annual discharge was only  $413 \text{ m}^3/\text{s}$ , resulting in N loads of 37,077 t/a and P loads of only 1,449 t/a. The close relationship

220 between discharge and nutrient loads is illustrated in Figs. 7b and c. This relationship emphasizes the dependency of annual riverine nutrient loads to the lagoon on the water discharge of the Oder River. The concentration of both nutrients, nitrogen

and phosphorus, is largely independent from river discharge. This has been observed already earlier and is the reason why the long-term assessment of critical loads used a discharge correction/normalization. Load reduction due to the changes in riverine

225 nutrient concentrations was more dominant in the 1990's (Friedland et al., 2019). The conclusion is that hydrological processes in the approximately  $120,000 \text{ km}^2$  Oder River catchment basin exert a stronger control over the nutrient loads to the Oder

Lagoon than annual changes in nutrient inputs. Consequently, future climate change effects on the catchment water budget will significantly impact the riverine nutrient loads and the ecological state of the lagoon. However, it is important to note that this conclusion may not apply to long-term perspectives, particularly when significant changes in the catchment begin to take effect.

In Germany, target or threshold values for a good ecological status in rivers exist, with concentrations below these values

230 indicating a good status. The riverine target values are 2.6 mg/L for nitrogen (N) and 0.1 mg/L for phosphorus (P). The nutrient

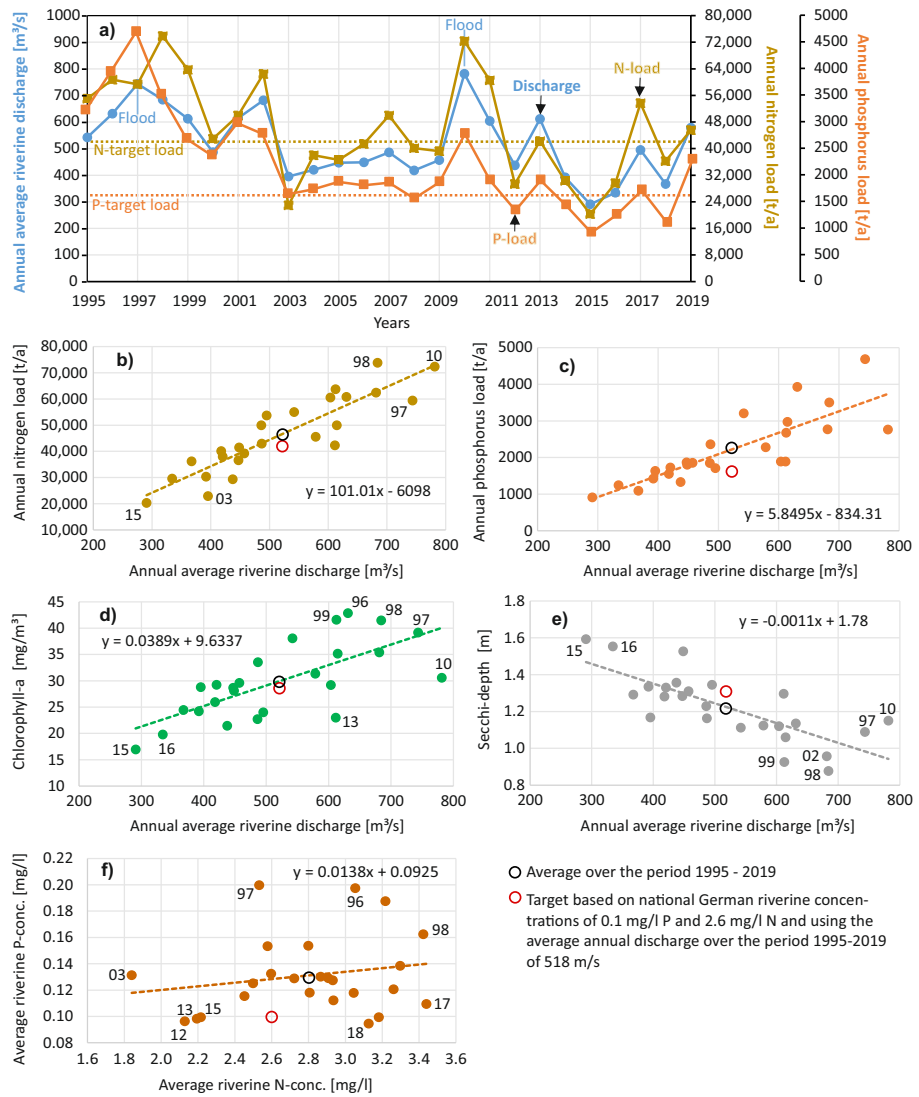


**Figure 7.** Average annual water discharge and annual loads of total nitrogen and total phosphorus to the Oder (Szczecin) Lagoon during a 25 years period (1995–2019), always including the rivers Oder/Odra, Uecker and Zarow. Relationship between riverine water discharge annual riverine nitrogen loads (b), annual riverine phosphorus loads (c), annual average phytoplankton biomass (chlorophyll-concentrations) (d) and annual average water transparency (Secchi depth) (e) in the Oder Lagoon (spatially integrated). (f) Relationship between riverine phosphorus and nitrogen concentrations. Panels b-e show highly significant correlations ( $p < 0.002$ ), while panel f demonstrates no significant relationship ( $p = 0.35$ ).

concentrations in recent years (2015-2019) were already close to these target concentrations. Using the average riverine water discharge to the lagoon of 518  $\text{m}^3/\text{s}$  (1995–2019) and the German nutrient target concentrations, the resulting target loads would be 42,506 t/a for N and 1,635 t/a for P. The HELCOM Baltic Sea Action Plan (BSAP) defines the maximum allowable

nutrient loads that enable the Baltic Sea to reach a good status. According to the BSAP, the maximum allowable loads are  
235 approximately 45,000 t/a for N and 1,500 t/a for P. Despite following different approaches, the German target values in rivers and the HELCOM maximum allowable loads result in comparable targets for the Oder River. In contrast, the Polish targets would allow much higher Oder River nutrient loads to the Oder Lagoon (63,661 t/a for N and 4,615 t/a for P), as shown by Friedland et al. (2019). However, during recent years (2015–2019), the N loads to the lagoon were 37,077 t/a and the P loads were 1,449 t/a. For both nutrients, the loads were below the maximum allowable inputs (HELCOM, 2013).

240 According to our model simulations, riverine nutrient loads have an immediate effect on major water quality indicators, namely phytoplankton biomass (chlorophyll-a) and water transparency (Secchi depth), and show a close correlation (Fig. 7d,e). Increased discharge, resulting in increased nutrient loads, causes an increase in chlorophyll-a concentrations in the lagoon and a decrease in Secchi depth. Calculated chlorophyll-a and Secchi depth values are average annual values over the entire lagoon and cannot be directly compared with existing ecological target values for central stations in the lagoon (Schernewski et al.,  
245 2015). However, the changes in chlorophyll-a concentrations and Secchi depth that would result from fully meeting the nutrient load targets (42,506 t/a N and 1,635 t/a P) are only minor (Fig. 7d,e). Compared to the average values over the period 1995–2019, chlorophyll-a concentrations would decrease by 5%, and Secchi depth would increase by 8%. Although, the nutrient loads are below the BSAP values, the lagoon remains in a highly eutrophic state with a bad ecological status, according to the official HELCOM HEAT HOLAS 3 (HELCOM, 2021b) eutrophication status assessment (BMU, 2024).

## 250 3.5 Interannual variability of discharge and loads and its consequences

The interannual variability of water discharge and nutrient loads is high (Fig. 7a). Annual discharges vary between 291m<sup>3</sup>/s in 2015, a dry and hot year, and 781m<sup>3</sup>/s in 2010, the year with one of the largest Oder River floods ever recorded, which occurred in May. Consequently, nutrient loads also show high variability, ranging from 20,309 t/a N in 2015 to 72,333 t/a N in 2010. For P, the range is from 4,683 t/a in 1997, another major river flood year, to 1,094 t/a in 2018, another hot and dry year. Over the 25-year period, riverine concentrations of N and P do not show a close relationship; the concentrations of both elements behave differently in different years .  
255 (Fig. 7f).

The differing interannual variability between N and P concentrations indicates that both nutrients enter via different pathways and that these pathways play different roles in different years. This suggests that seasonal discharge and nutrient emission  
260 patterns need to be analyzed separately and in depth. It is likely that the interannual variability is controlled by extreme events lasting weeks to a few months, which can strongly affect the annual values and the lagoon ecosystem.

The Baltic Sea environment is projected to experience extreme conditions more frequently in the future (Rutgersson et al., 2022). These include, but are not limited to, increased occurrences of flooding and drought events. Given that these events substantially influence nutrient loads, they are likely to amplify the interannual variability of ecological conditions. Consequently,  
265 the increased amplitude of environmental fluctuations will intensify stress on lagoon fauna and flora.

## 4 Discussion

### 4.1 Quality of the model results Model performance and limitations

The Oder Lagoon model demonstrates strong performance in simulating physical and biogeochemical processes. The assessment was conducted at two central stations located in the lagoon's subregions Kleines Haff (western part) and Großes Haff 270 (eastern part), where the best coverage of observations was available.

The model successfully reproduces temperature and salinity patterns at both sites, particularly capturing the interannual salinity variability. However, it fails to replicate the highest observed salinity values. We attribute this limitation to the truncated Dziwna channel in the model (Fig. A6), which results in overestimated transport through the Dziwna channel at the expense of 275 transport through the Swina channel, thereby introducing less saline water into the lagoon. Additional uncertainty stems from the meteorological forcing and consequently the open boundary conditions.

Transport estimates through the connecting channels (Mohrholz and Lass, 1999) suggest that mass transport in the Peene and Dziwna channels is equal, or possibly even lower in the Dziwna channel. However, our simulation yields a mass transport 280 in the Dziwna channel that is twice that of the Peene channel. One possible explanation for this discrepancy could be the incomplete representation of the Dziwna channel in our lagoon bathymetry (see Fig. 1). The absence of the Dziwna channel's full hydraulic resistance in the model could account for the enhanced mass transport observed in the simulation.

A notable characteristic of the simulated nutrient concentrations is the absence of extremely high phosphate values (Fig. A7). It is hypothesized that these high values are caused by the release of sedimentary phosphate under low-oxygen conditions. Although this process is included in the model (Fig. A8), the amount of phosphate released is evidently insufficient to elevate 285 the surface concentration to observed levels. This discrepancy could be attributed to the two-dimensional sediment module used in this study. This kind of model does not have a long memory in terms of, for example, the storage of iron-phosphate complexes. Therefore, our model does not 'remember' the peak eutrophication period in the 1980s and early 1990s. A hint for this explanation is the reduced phosphate peak frequency in recent years. Implementing a more sophisticated, vertically resolved sediment module (Radtke et al., 2019) could potentially improve the model's performance.

Oxygen Model simulations show that near-bottom oxygen deficiency in the near-bottom water is widespread in the Oder Lagoon 290 occurs as widespread, episodic events. The most affected area is the artificial navigation channel (see Sec. 3.2). In the recent model implementation, the model does not account for ship traffic, which causes regular vertical mixing down to the bottom. Thus, in contrast to the model, observations do rarely show hypoxia in the navigation channel. Given that the navigation channel constitutes only a small fraction of the Oder Lagoon's total area, these localized oxygen dynamics have minimal impact on the overall phosphate release and binding processes in the lagoon system.

The eastern part of the lagoon experiences anoxia more frequently and for longer periods. This is caused by the high nutrient loads from the Oder River entering this part of the lagoon (Fig. 295 1).

To the best of our current knowledge, no direct observations of anoxic conditions in the Oder Lagoon have been documented.

300 This absence of empirical data can primarily be attributed to suboptimal temporal and spatial sampling strategies. Nevertheless,

**Table 2.** The mean relative biomass of model phytoplankton groups, averaged over the 25-year simulation period (1995–2020), illustrating the lagoon's phytoplankton community structure.

Phytoplankton group	Carbon biomass [mol]	Share [%]
Limnic phyto.	269558	92
Large cell phyto.	10083	3.4
Small cell phyto.	258	0.2
Cyanobacteria	12839	4.4

several proxy indicators suggest episodic anoxia occurrence, including documented fish and mussel mortality events as well as summer phosphate peaks. These findings have been comprehensively reported in Schernewski et al. (2025b).

The newly introduced phytoplankton functional group (limnic phytoplankton) is by far the most abundant model phytoplankton group (Tab. 2). This new group was necessary to achieve realistic biomass concentrations. In the lagoon. The limnic group's adaptation to low-light, CDOM-rich conditions enables realistic phytoplankton biomass simulation in the model. In environments outside the lagoon, where salinity levels are substantially higher, the limnic phytoplankton group becomes effectively absent from the community composition. This exclusion results from growth limitations imposed by elevated salinity conditions, which exceed the group's threshold. This mechanism, in combination with the other three groups, we ensure that allows us to apply the biogeochemical model ERGOM can be applied in coastal waters of the Baltic Sea as well as in the open Baltic Sea without parameter tuning. This is especially important when the model is set up for the entire Baltic Sea at a high spatial resolution, for example, one nautical mile 2 km or finer, where lagoons are partly resolved. In this case, the ecosystem model provides reasonable results in coastal waters, lagoons, and the open Baltic Sea. We applied this Baltic Sea model to create open boundary conditions for the Oder Lagoon model, ensuring proper domain connectivity with the larger Baltic Sea model. Thus, simulations with a coarse-grained model deliver nearly seamless data for the open boundaries of the local model setups.

Further discussion of the model performance is provided in Appendix A.

## 4.2 Filter function for nutrients

An important ecological function of the Oder Lagoon is, *inter alia*, the filtration and retention of nutrients. Acting as a system between the Oder River mouth and the Baltic Sea, it reduces the amount of nutrients entering the open Baltic Sea. Budget calculations based on observations in Lampe (1999) yield a low retention capacity of 2%–5%, mainly caused by dredging of the navigation channel. Grelowski et al. (2000) found with a similar method that 12%–29% of total nitrogen and 11%–27% of total phosphorus is retained in the Oder Lagoon. Asmala et al. (2017) compiled removal rates (burial and denitrification) from coastal systems around the Baltic Sea and analyzed their spatial variation. They showed that denitrification in lagoons of the Baltic Sea is highest, while phosphorus burial in lagoons is small compared to other coastal systems. Our model based approach yields a retention capacity of 40% for nitrogen and 12% for phosphorus. The lower retention for phosphorus is in line with Asmala et al. (2017). In contrast to Asmala et al. (2017), who only considered sedimentary denitrification, we considered additional sources and sinks for nitrogen: nitrogen fixation, pelagic denitrification, and nitrogen burial. However, burial and pelagic denitrification are only minor contributions to the nitrogen retention.

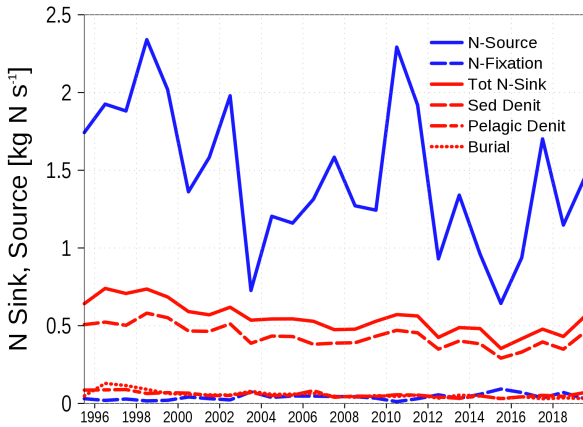


**Figure 8.** Nitrogen sources (blue) and sinks (red) in the Oder Lagoon. N-Sources are riverine loads and atmospheric deposition while N-Fixation is shown as a separate source (blue, dashed line). Tot N-Sink is the total sink of nitrogen; Red dashed and dotted lines are the contributing processes.

(Tab. 1).

330 Pastuszak et al. (2005) use observations for budget calculations and report substantially higher retention rates of 85% for nitrogen and 72% for phosphorus. However, these elevated values must be interpreted with consideration of methodological differences: their study encompassed inland regions of the Oder Lagoon that extend beyond our defined model domain, potentially influencing the observed retention metrics.

335 Figure 8 illustrates the nitrogen sources and sinks in our model. The dominant source is riverine nutrient loads, while the primary sink is denitrification in the sediment. Dredging is not included in the model. However, its absence is nearly compensated for by the model's sediment burial process, which occurs when the sediment thickness exceeds a specified threshold. The only sink for phosphorus is sediment burial as shown in Tab. 1.

340 Models offer the advantage of enabling experiments to be performed on the system. We conducted an experiment with halved riverine nutrient loads. The reduced loads resulted in decreased retention for phosphorus, while the retention for nitrogen increased (see Fig. 4). The cause of the lesser phosphorus retention is the reduced primary production due to lower nutrient concentrations. This, in turn, leads to less sedimentation and hence, less burial. However, this dependence is not statistically significant based on our model simulations. Simulations with a broader range of loads could potentially establish a statistically significant relationship if it exists. Nevertheless, the loads we applied are within a reasonable range for realistic scenarios. In the case of nitrogen, the contributing sinks behaved differently (see Fig. 9). While burial is reduced, similar to the phosphorus case, the relative sedimentary denitrification increases. Denitrification in the sediment is more effective with higher oxygen concentrations at the sediment-water interface. The higher oxygen concentration results from less primary production due to

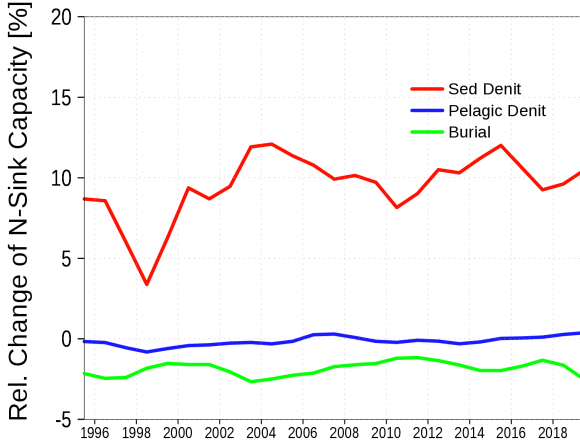


**Figure 9.** Change in relative nitrogen retention capacity between control run and 50% load reduction run.

reduced loads and hence less organic matter sinks to the sediment. Overall, nitrogen retention is more effective in the case of lower nutrient loads. A significant correlation ( $p < 0.001$ ) could be established for this relationship (Fig. 5b).

Coarse-resolution models, commonly employed for basin-wide, long-term simulations of the Baltic Sea, typically lack the spatial resolution necessary (on the order of 1 km or finer) to adequately capture coastal hydrodynamic features and associated biogeochemical processing (i.e., the coastal filter function). For river systems discharging into lagoons prior to reaching the open Baltic Sea, particularly large rivers with substantial nutrient inputs, we therefore recommend implementing load correction procedures.

Current state-of-the-art approaches typically apply empirically-derived bioavailability factors, determined through model calibration, to account for coastal nutrient retention. However, these conventional methods present several limitations:

- They generally employ globally uniform factors that neglect the heterogeneity of coastal filter systems
- They assume temporal constancy, ignoring potential variability in retention efficiency

Our proposed mechanistic approach offers two key advantages:

- Enhanced regional Realism: By explicitly quantifying lagoon-specific retention capacities using high-resolution local models, we generate more accurate, spatially-resolved nutrient load estimates
- Improved model performance: The mechanistic representation of retention processes facilitates more realistic ecosystem model calibration, potentially reducing compensatory errors in other model components

This mechanistic approach necessitates quantitative assessment of lagoon retention capacities through dedicated, high-resolution local modeling efforts. Particular emphasis should be placed on characterizing load-dependent variability in retention efficiency, as nutrient processing rates often exhibit nonlinear responses to input concentrations.

For comparable coastal filter systems, particularly lagoons, established empirical relationships (e.g., retention capacity as a function of water residence time) may serve as valuable initial approximations. Such relationships provide scientifically grounded starting points that can be subsequently refined through site-specific high-resolution local modeling effort.

In summary, the filter function appears as follows: The fraction of nitrate removal is larger than that for phosphorus. A 370 dependence of the retention rate on loads exists for nitrogen. An additional dependence exists on the Additionally, both nitrogen and phosphorus retention show significant dependence on water residence time. For phosphorus, we did not find a similar dependence. in the lagoon system. We think that these findings can be transferred to similar coastal regions like the Curonian Lagoon, especially the dependence of the nitrogen nutrients removal rate on the water residence time. However, transferring our findings to other regions requires additional sound scientific studies. This is particularly true for semi-enclosed and open coastal systems.

### 375 4.3 Implications for water quality

Our 25-year simulation (1995-2019) indicates mean annual nutrient exports from the Oder Lagoon to the Baltic Sea of 28,988 tonnes for nitrogen and 1,945 tonnes for phosphorus. When accounting for these retention-mediated reductions, the resulting nutrient loads to the Baltic Sea consistently remained below the target thresholds established by the Baltic Sea Action Plan (BSAP) throughout the simulation period. However, the Oder Lagoon case demonstrates that achieving water quality targets in 380 connected river systems and the Baltic Sea does not necessarily translate to good ecological status in transitional water bodies, highlighting the need for ecosystem-specific management approaches.

A good ecological status in the lagoon would require significant additional nutrient load reductions and the implementation of measures in the river catchment at high and likely unrealistic costs. It is likely that the lagoon must be regarded as a naturally eutrophic ecosystem with limited management possibilities. A re-evaluation of water quality targets in the lagoon requires a 385 more detailed study that includes neighboring coastal waters to address interrelationships, relates model data to field data with a focus on the assessment stations, and carefully considers evaluation aspects such as water depth and evaluation period.

## 5 Conclusions

We developed a local model for the Oder Lagoon that realistically reproduces its physical and biogeochemical properties. This model serves as a tool for conducting studies in this area and, specifically, for quantifying the lagoon's nutrient retention 390 capacity. This is a crucial step in adjusting riverine loads for coarse-grained models, which often do not adequately resolve lagoons. Our approach can be readily applied to other lagoons in the Baltic Sea, such as the Curonian Lagoon, and can also be adapted for regions beyond the Baltic Sea. A general finding is the relationship between water residence time and retention of nitrogen.

The analysis shows that the nutrient retention in the lagoon already reduces nutrient loads to the open Baltic Sea in agreement 395 with the BSAP (Table 3). Furthermore, riverine loads into the Oder Lagoon also meet the German targets for the Oder River. However, nutrient concentrations in the Oder Lagoon do not achieve the intended target values for good ecological status. This

**Table 3.** Loads for different periods and targets into the Oder Lagoon and Baltic Sea. Loads and targets are in kt/a, runoff in  $\text{m}^3\text{s}^{-1}$ . N and P retention is estimated from the period 1995 to 2019. Loads to the Baltic Sea for other periods are estimated from the mean retention.

	N-load Lagoon	N-load Baltic	P-load Lagoon	P-load Baltic	Runoff	N-retention	P-retention
1995–2019	46,266	28,988	2,198	1945	518	0.37	0.12
1995–1999	62,534	39,181	3,600	3,186	643		
2015–2019	31,077	23,231	1,449	1,282	413		
German target Oder River	42,506		1,635				
BSAP MAI to Baltic		45,000		1,500			

points to the problem that quality standards for inner and outer waters are not harmonized, making it unrealistic to achieve a good ecological status for the Oder Lagoon.

The simulation data generated in this study enable several additional analyses that could be the focus of future studies. 400 For example, these could include short- and long-term responses to extreme events such as floods and droughts. Further improvements should include a more realistic representation of the Dziwna channel length and coupling the model with a more advanced sediment module than the one used in this study. Another weakness is the lack of ventilation of the deep water in the navigation channel due to ship traffic, which should be properly parameterized in an upcoming model version.

To complement our hindcast simulations, targeted scenario analyses could provide valuable insights into the system's sensitivity 405 to specific anthropogenic interventions. Particularly informative scenarios might include:

- (a) Assessments of varying ship traffic intensities and their impacts
- (b) Evaluations of potential navigation channel deepening effects

Such scenario simulations would enable a more comprehensive understanding of the lagoon's response to management measures and environmental modifications.

410 *Code and data availability.* Observations from the Oder Lagoon monitoring program were provided upon request by the German State Agency for Environment, Nature Conservation and Geology Mecklenburg-Vorpommern (Mario von Weber, LUNG-MV) and Główny Inspektorat Ochrony Środowiska (Adam Czugała). Nutrient loads and runoff data for the Oder River were obtained from the Polish Główny Inspektorat Ochrony Środowiska. Corresponding data for the rivers Zarow and Ücker were available from LUNG-MV.

The meteorological forcing is archived at [https://doi.org/10.1594/WDCC/coastDat-2\\_COSMO-CLM](https://doi.org/10.1594/WDCC/coastDat-2_COSMO-CLM) (last access: 26 November 2024, 415 Geyer and Rockel (2013)).

All model output that was analyzed in this paper, the model code, and data to run the model has been published at <https://doi.org/10.5281/zenodo.14236528> (Neumann et al., 2024).

## Appendix A: Detailed analysis of the model performance

In this section, we compare model data with observations, demonstrate some model properties not present in observational data,

420 and discuss the results of this analysis. Observations are available on request from national agencies (see *data availability*).

### A1 Station data

#### A1.1 Climatology

We start with the evaluation of data from stations KHM and C shown in Fig. 1. Figure A1 shows the climatologies (1996-2019)

425 for several surface variables and bottom oxygen. The model is able to reproduce the observations, and the spread of the model

and observations mostly matches. However, a few details need to be mentioned and discussed.

The Oder Lagoon was covered by sea ice in several winters during the simulation period. No observations exist for these time periods. Thus, cold temperatures are missing in the observational dataset, and the number of winter values for nutrients is reduced.

The model overestimates the summer temperature and underestimates the salinity. Several reasons could be responsible for

430 these biases. However, within the scope of this study, we cannot verify which factors drive the observed biases. Thus, we can only suggest some possibilities that could be the subject of further investigations. (i) The meteorological forcing impacts both temperature and salinity, and in addition, the mixing depth. A mixing depth that is too shallow could also be responsible for

435 the positive temperature bias in summer. Beyond the meteorological forcing, the choice and tuning of the vertical sub-scale parameterization determines the mixing depth. Observations are only available for the surface and bottom layers. Thus, there is

435 hardly any constraint for the mixing depth. For salinity, the freshwater budget in the lagoon is also an important factor, which is controlled by the Oder River discharge (Sec. 3.4). The overestimated volume transport through the Dziwna channel (Sec. A1.2) may also contribute to the lower salinity values in the model.

The observed chlorophyll has two distinct peaks, denoting spring and late summer blooms. In the model, only one peak

440 appears in early summer. Chlorophyll is not a model's state variable and is diagnostically estimated with a constant carbon-

to-chlorophyll ratio. It is well known (Jakobsen and Markager, 2016) that this ratio has a seasonal cycle, which we do not consider (see our remarks in Sec. A1.2). Another limitation of our simulations is the systematic underestimation of winter

445 opacity (Fig. A3), which may potentially advance the timing of vernal blooms. This discrepancy likely arises from our model's current implementation, which accounts for resuspension of organic matter only, while neglecting the resuspension of mineral sediments. The omission of mineral sediment dynamics probably contributes to the simulated overestimation of winter water

clarity.

For our near-bottom oxygen comparisons, we utilized model data from 1 meter above the seafloor, corresponding directly to the standard observational measurement depth. However, we note that oxygen concentrations in our highest-resolution model output (20 cm above the seafloor) are systematically lower. This vertical gradient is consistent with recent findings by

Fredriksson et al. (2024), who demonstrated that strong oxygen gradients commonly exist in the bottom boundary layer of

450 coastal systems - gradients that typically exceed the resolution capabilities of conventional CTD instrumentation. Additionally,

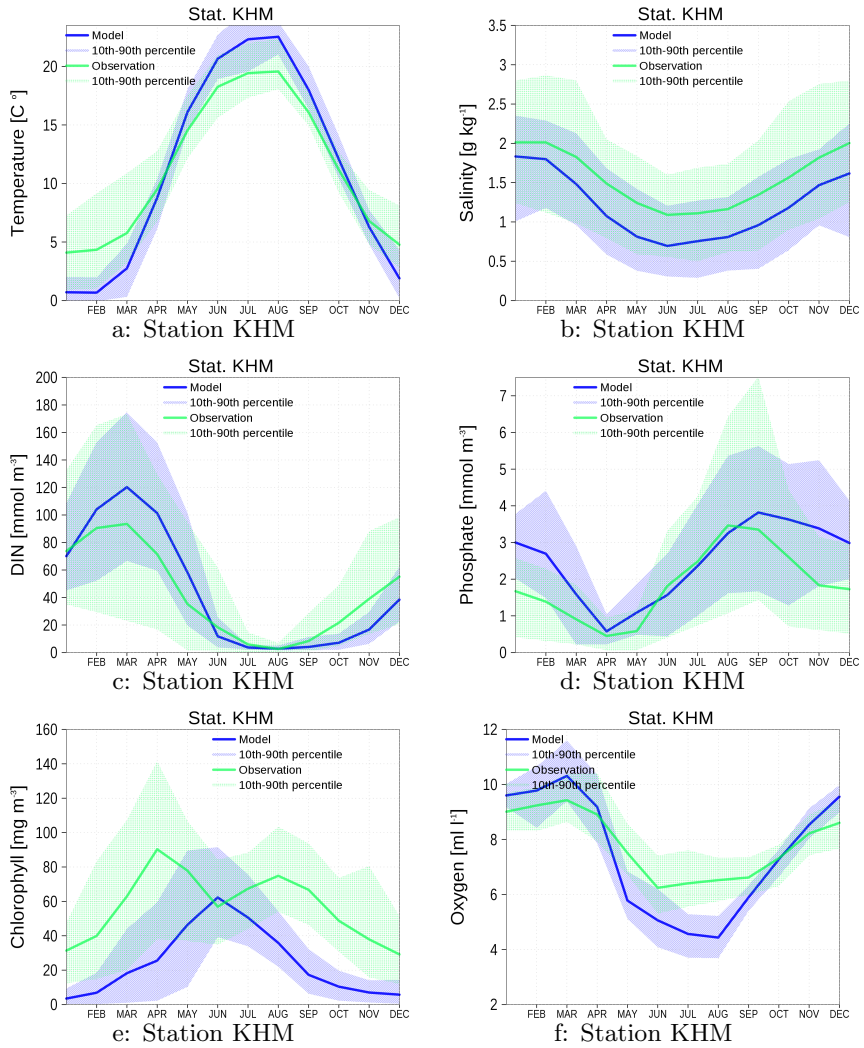


**Figure A1.** Climatology of surface data for temperature (a), salinity (b), DIN (c), phosphate (d), and chlorophyll (e). Bottom oxygen is shown in (f). Blue color are data from the model green color are data from observations. The shaded area is the range between 10th and 90th percentile. All data are from station KHM (see Fig. 1).

we acknowledge that traditional measurement platforms (typically research vessels) may introduce artifacts by disrupting the natural vertical stratification of the water column during sampling operations. Our model-data comparison at 1 m above the seafloor reveals a slight negative bias in simulated oxygen concentrations. Despite this, our analysis confirms that within the 10th-90th percentile range of observations, anoxic conditions are never encountered, indicating persistent oxic conditions and

455 stable redox potential throughout most of the study period. While anoxic events remain rare and temporally limited in this system, these episodic occurrences exert disproportionate influence on:

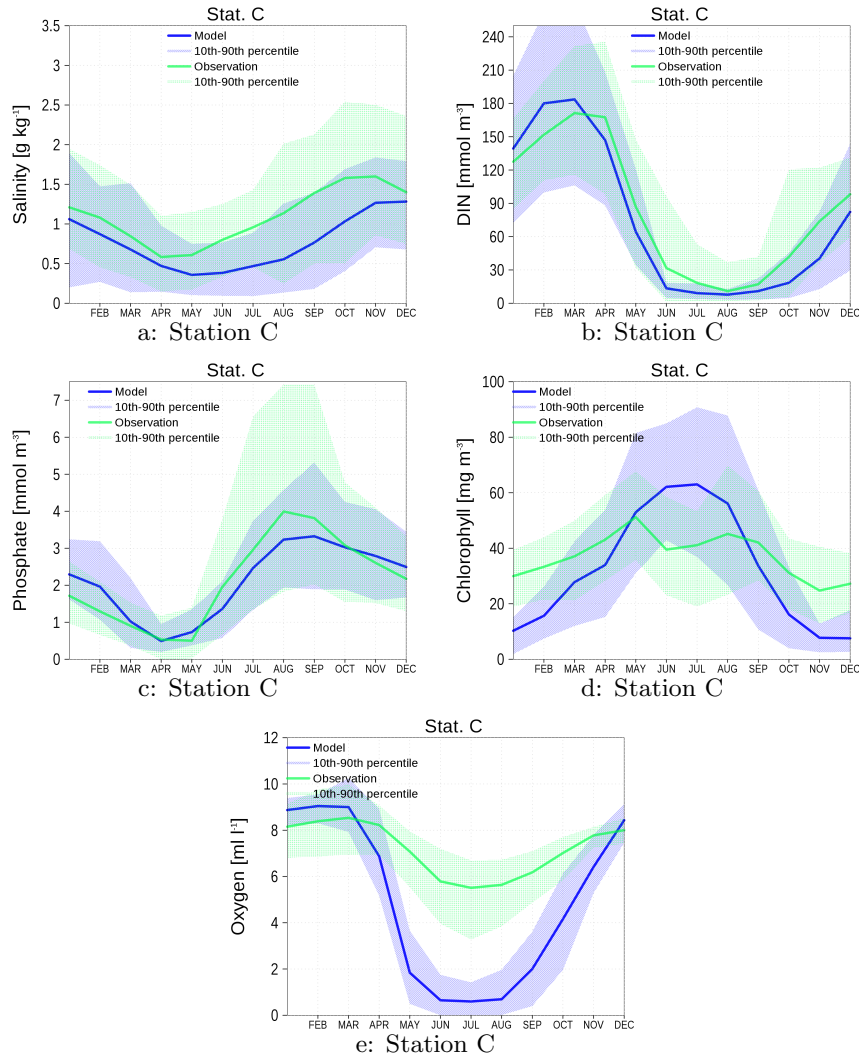


**Figure A2.** Climatology of surface data salinity (a), DIN (b), phosphate (c), and chlorophyll (d). Bottom oxygen is shown in (e). Blue color are data from the model green color are data from observations. The shaded area is the range between 10th and 90th percentile. All data are from station C (see Fig. 1).

- Phosphorus biogeochemical cycling
- Benthic community structure and function

Notably, these conclusions remain robust even when considering our highest-resolution near-bottom simulation data (20 cm  
460 above the sediment-water interface, not shown).

The assessment for station C (Fig. A2) mirrors that of station KHM. Unfortunately, temperature data are unavailable for this station. Simulated bottom oxygen levels are lower than those at station KHM, which can be attributed to the greater water depth

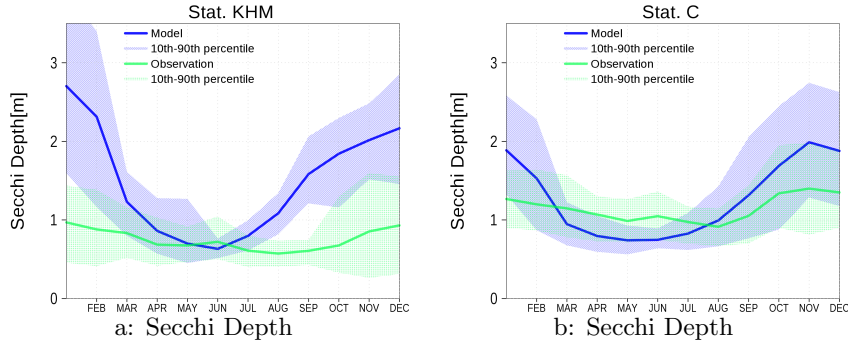


**Figure A3.** Climatology of Secchi depth at stations KHM (a) and C (b) (see Fig. 1).

**Table A1.** Root mean square error (RMSE), standard deviation (STD) of the observations, and normalized RMSE (RMSD).

	RMSE	STD	RMSD
DIN KHM	36	44	0.8
DIP KHM	1.6	1.6	1.0
Salt KHM	0.56	0.69	0.82
Temp KHM	3.3	6.3	0.5
DIN C	47	67	0.7
DIP C	1.4	1.7	0.8
Salt C	0.59	0.65	0.9

in the navigation channel. The model does not incorporate the substantial ship traffic to and from Szczecin harbor. According to Schernewski et al. (2025a), approximately 3,300 cargo ships arrive at Szczecin harbor annually. The deep draught of these vessels, which nearly reaches the seafloor in the navigation channel, induces regular mixing of the water column.

Another difference between the model and reality involves the dredging of the navigation channel. Functioning as a sediment trap, the channel requires regular dredging to maintain its depth (Schernewski et al., 2024). While the model's burial process partially simulates this dredging effect, it represents only an approximation of the actual process.

Figure A3 presents the climatology of Secchi depth at stations KHM and C. The model data demonstrate more pronounced seasonality compared to the observations. This discrepancy may stem from the model's exclusion of mineral sediment particles. The resuspension of these particles, particularly during winter when wind mixing is stronger, serves to limit Secchi depth. Additionally, it is important to note the absence of data during sea ice winters.

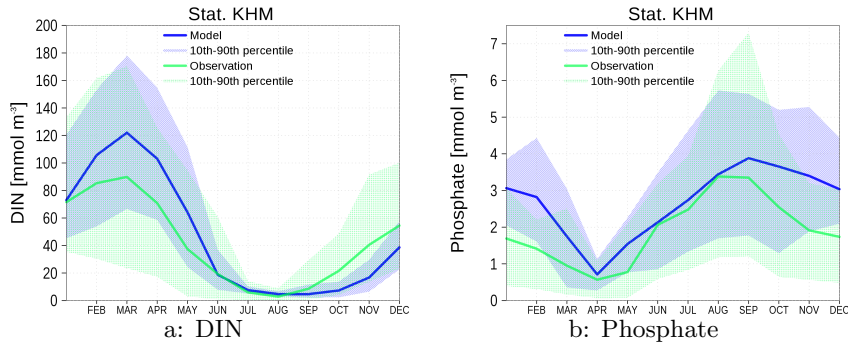


**Figure A4.** Bottom DIN and phosphate station KHM (see Fig. 1). The shaded area is the range between 10th and 90th percentile.

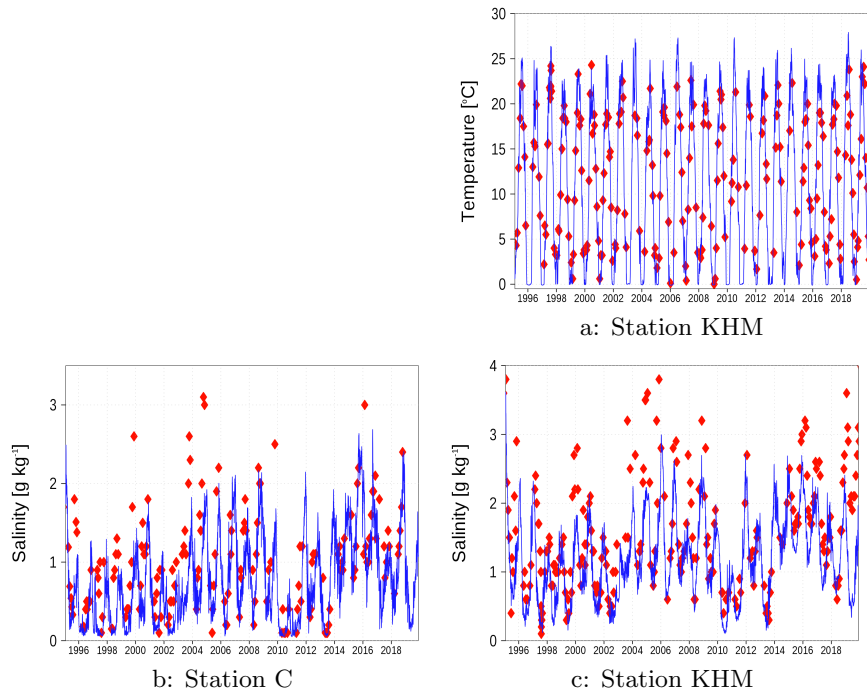
Finally, Table A1 presents the root mean square error (RMSE) and the RMSE normalized by the standard deviation of observations (RMSD). An RMSD value below unity indicates that the RMSE falls within the range of natural variability (Kärnä et al., 2021).

For completeness, we have included Fig. A4, which compares simulated and observed near-bottom nutrient concentrations at stations KHM. Notably, these near-bottom values exhibit minimal divergence from surface concentrations (Fig. A1), suggesting frequent vertical homogenization of the water column. This interpretation is further supported by Fig. A8, which demonstrates that stratification events in the Oder Lagoon are typically short-lived and frequently disrupted by meteorological forcing.

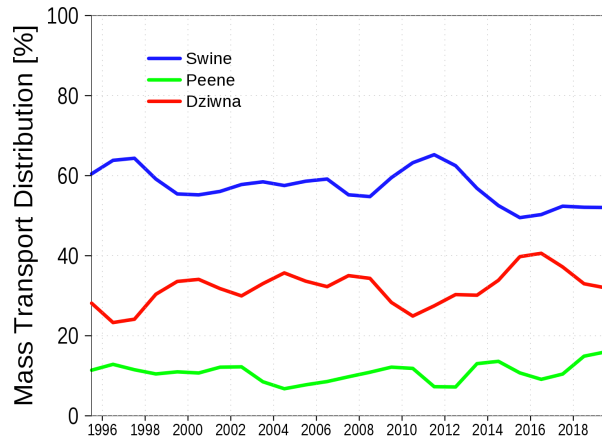
#### 480 A1.2 Time series

Figure A5 presents surface salinity measurements at stations C (panel b) and KHM (panel c). The simulations at both stations successfully capture the observed interannual variability, though the model exhibits a negative salinity bias for some periods. Corresponding sea surface temperature (SST) data are shown in Figs. A5a for station KHM. Winter observations are frequently unavailable due to sea ice coverage, while during summer months, the model tends to overestimate SST values compared to observations.

Water exchange between the lagoon and the Baltic Sea occurs through three primary channels: the Peene Stream, the Świna, and the Dziwna (Fig. 1). The relative contribution of each channel to the overall water exchange with the Baltic Sea has been estimated in multiple studies using both observational data and modeling approaches. Mohrholz and Lass (1999) provides a comprehensive overview of these estimates, reporting the following contribution ranges: Peene Stream: 14%–20%, Świna: 60%–75%, and Dziwna: 9%–20%. Figure A6 illustrates the contributions of the three channels to water exchange in the model simulation. The transport through the Dziwna channel appears higher than in other estimates, while transport through the Świna channel is reduced. This discrepancy occurs because the truncated Dziwna channel reduces hydraulic resistance. This issue should be addressed in future, improved model setups.



**Figure A5.** Surface temperature and salinity at station KHM (a,c) and salinity at station C (b) (see Fig. 1). Red diamonds: Observations; Blue line: Model simulation.



**Figure A6.** The relative contribution of the three outlet channels of the Oder Lagoon to the net water exchange with the Baltic Sea.

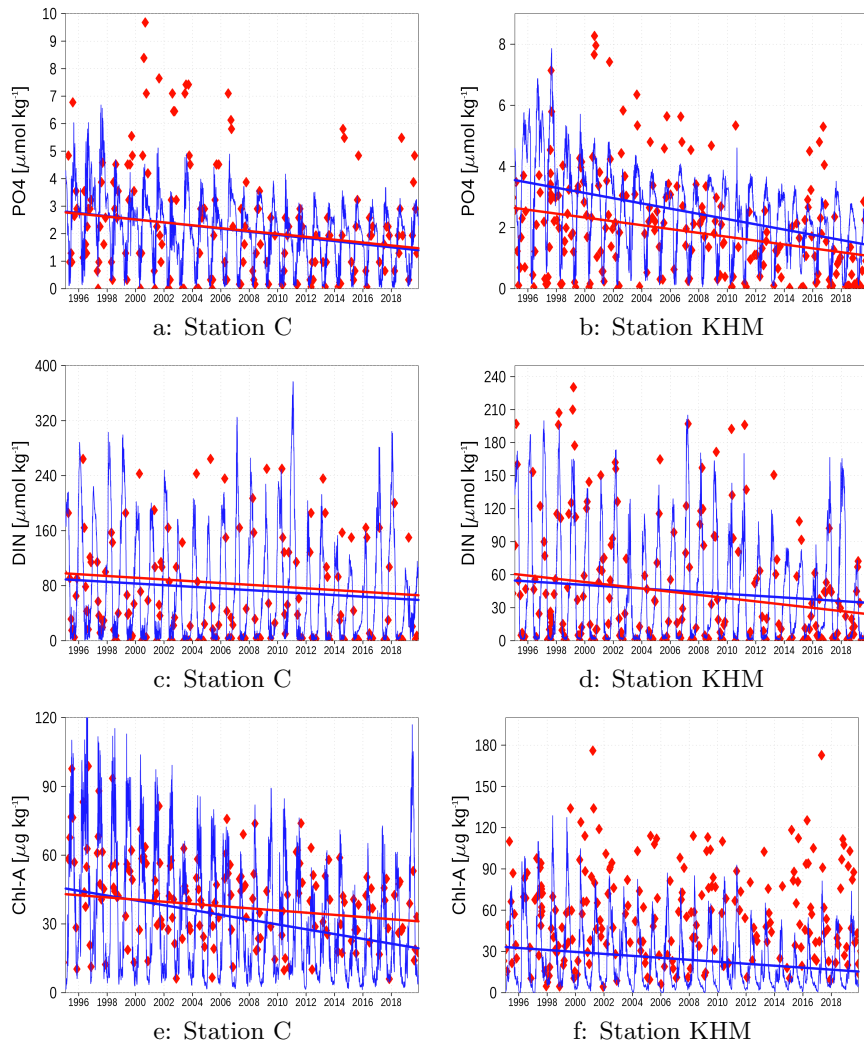


**Figure A7.** Surface concentration of phosphate, DIN, and chlorophyll at station C (a,c,e) and station KHM (b,d,f) (see Fig. 1). Red diamonds: Observations; Blue line: Model simulation. Straight lines show the trend if significant.

Figure A7 presents time series of nutrient concentrations, including phosphate, dissolved inorganic nitrogen (DIN), and chlorophyll, at stations C and KHM. The model successfully captures the decreasing trend in winter phosphate concentrations at both stations. However, it fails to reproduce the exceptionally high observed concentrations during summer months. These peak values are assumed to result from very low oxygen conditions at the sediment surface, which liberate iron-bound phosphate from the sediment. Although this process is included in the model, the amount of phosphate released is insufficient to significantly elevate surface concentrations. In certain periods and regions, the model indicates oxygen depletion (see Sec. 3.2), suggesting that the preconditions for phosphate release are indeed met. We hypothesize that the two-dimensional

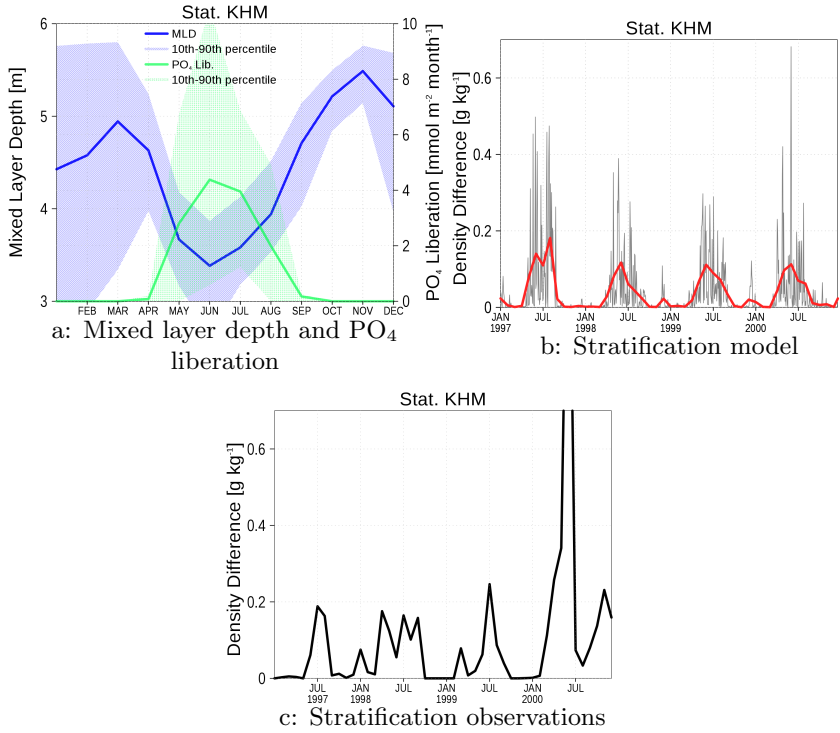


**Figure A8.** Climatology of model mixed layer depth and PO<sub>4</sub> liberation (a), stratification in model simulation (b), and in observations (c). Blue color in (a) are the mixed layer depth and green color the PO<sub>4</sub> liberation. The shaded area is the range between 10th and 90th percentile. The red line in (b) is from monthly mean and the black line from two-day mean model data. For (c), monthly mean observations are used. All data are from station KHM (see Fig. 1).

sediment module of the ERGOM model cannot sufficiently parameterize vertical processes, which might be important for the long-term storage of phosphorus in the sediment.

The model underestimates chlorophyll concentrations at station KHM. This discrepancy may be attributed to our simple chlorophyll estimation method, which uses a constant Chl:C mass ratio (see section 2). This approach neglects the annual dynamics of the Chl:C ratio, which represents a phytoplankton response to changing ambient light conditions and Chl:C may vary between 23 and 60 (Jakobsen and Markager, 2016). Furthermore, the simulated data exhibits a slight decreasing trend, whereas the observations at station KHM do not display a significant trend.

## A2 Stratification and phosphorus liberation from sediments

Particulate iron-phosphate complexes, primarily accumulated in sediments, dissolve under anoxic conditions, consequently liberating phosphate from the sediment. This process, also known as internal eutrophication (Vahtera et al., 2007), is included in our ecosystem model ERGOM, as demonstrated in Fig. A8.

515 The mixed layer depth reaches its minimum in summer, coinciding with strong stratification that results in low bottom oxygen concentrations (Fig. A1f). Simultaneously, phosphate is liberated from sediments (Fig. A8a), yielding maximum phosphate concentrations in summer (Figs. A1d and A2c). However, this summer phosphate peak is less pronounced in the model compared to observations.

520 Mixed layer depth cannot be derived from observations because only surface and near-bottom data are available. Instead, we present the density differences between bottom and surface water as a measure of stratification in Fig. A8b,c. Observations are compiled as monthly data, which can be compared to the red line in Fig. A8b. The higher values of the two-day means (black line) indicate that strong stratification, and potentially anoxia, occurs in the form of discrete events. For visual clarity, we focus the analysis on the period from January 1997 to December 2000.

525 Our comparative analysis demonstrates strong agreement between observed and simulated stratification patterns, with both datasets showing peak stratification intensity during summer months. Given that stratification constitutes a necessary precondition for anoxia development, this correspondence demonstrates that both the natural system and our model have the potential to develop anoxic conditions under appropriate circumstances.

### 530 525 **A3 Horizontal patterns**

Simulated data are evaluated against monitoring data, enabling the calculation of the root mean square deviation (RMSD) for each station and parameter. Following Kärnä et al. (2021), we normalize the root mean square error by the standard deviation of the observations to facilitate comparisons across different stations and parameters. A dimensionless normalized RMSD value below one is typically considered indicative of good model performance, as it suggests that the RMSD falls within the range 530 of natural variability observed in the data.

Figure A9 presents horizontal surface patterns of model variables and their corresponding RMSD. For the winter season, observations were unavailable for all stations. Dissolved inorganic nitrogen (DIN) exhibits a clear gradient in both seasons, with the highest values near the mouth of the Oder River and concentrations decreasing sharply toward the western lagoon and the open Baltic Sea. The RMSD for the monitoring stations is predominantly below one, indicating good model performance. 535 Only at station E (near the mouth of the Oder River) does it slightly exceed this threshold.

Dissolved inorganic phosphorus (DIP) displays an opposite gradient during winter, with the highest concentrations in the western lagoon. During the growing season, DIP concentrations remain elevated. While the RMSD during the growing season is mostly below one (except at station E near the Oder River), the model overestimates DIP concentrations in winter compared to observed values. For the remainder of the year, DIP concentrations fall within the range of observations (see Figs. A1 and 540 A2).

Summer chlorophyll-a concentrations and Secchi depth (Fig. A9) exhibit comparable gradients due to their close relationship. The lowest chlorophyll-a concentrations occur in the western part of the lagoon, where Secchi depth is greatest. Although chlorophyll-a is underestimated in the western part, the RMSD remains within the range observed at eastern stations. For Secchi depth, the RMSD is even better for western stations (values between 1.1 and 1.2), while it reaches up to two for eastern 545 stations. Despite the good agreement between modeled and observed chlorophyll-a in the eastern Oder Lagoon, the model

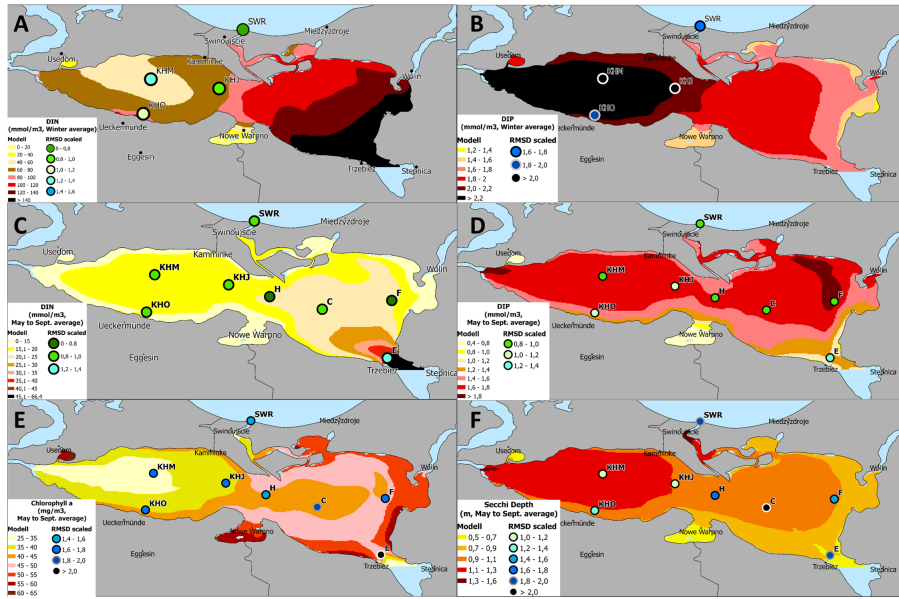


**Figure A9.** Near surface concentrations of dissolved inorganic nitrogen A: Winter average, C: May to September average; dissolved inorganic phosphorus B: Winter average, D: May to September average; Chlorophyll-a E: May to September average, and Secchi depth F: May to September average. All parameters are averaged from 2010 to 2019. The model results are color-coded and circles indicate the normalized RMSD for each monitoring station and parameter. The map was created using the software ESRI ArcGIS Pro (Version 3.3.2; <https://pro.arcgis.com>).

simulates too rapid a decline in chlorophyll-a at station C during September, resulting in an overly rapid increase in Secchi depth during that month (see Fig. A2). Additionally, the model does not account for resuspended mineral sediments, which impact Secchi depth as outlined in Sec. A1.1.

*Author contributions.* TN set up the model and conducted the simulations. All authors contributed to the study design, data analysis, and the writing of the manuscript.

*Competing interests.* The corresponding author has declared that none of the authors have any competing interests.

*Acknowledgements.* The authors gratefully acknowledge the computing time made available to them on the high-performance computer "Emmy" at the NHR Center NHR-NORD@GÖTTINGEN. This center is jointly supported by the Federal Ministry of Education and Research and the state governments participating in the NHR ([www.nhr-verein.de/unsere-partner](http://www.nhr-verein.de/unsere-partner)). We thank LUNG-MV (Mario von Weber)

555 and Główny Inspektorat Ochrony Środowiska (Adam Czugała) for providing German and Polish monitoring data. This work was financially supported by the German Federal Ministry of Education and Research, projects “Coastal Futures II” (grant number 03F0980B), “Prime Prevention” (grant number 03F0953D) and UBA-MoSea (FKZ 3723252040). We acknowledge the contributions of Sarah Piehl, who collected and prepared data from German and Polish authorities.

## References

560 Zustand der deutschen Ostseegewässer 2024, Bundesministerium für Umwelt, Naturschutz, nukleare Sicherheit und Verbraucherschutz (BMUV) (Hrsg.), [https://mitglieder.meeresschutz.info/de/berichte/zustandsbewertungen-art8-10.html?file=files/meeresschutz/berichte/art8910/zyklus2024/Zustandsbericht\\_Ostsee\\_2024.pdf](https://mitglieder.meeresschutz.info/de/berichte/zustandsbewertungen-art8-10.html?file=files/meeresschutz/berichte/art8910/zyklus2024/Zustandsbericht_Ostsee_2024.pdf), (last access: 2024-11-20), 2024.

Almroth-Rosell, E., Edman, M., Eilola, K., Meier, H. E. M., and Sahlberg, J.: Modelling nutrient retention in the coastal zone of an eutrophic sea, *Biogeosciences*, 13, 5753–5769, <https://doi.org/10.5194/bg-13-5753-2016>, 2016.

565 Asmala, E., Carstensen, J., Conley, D. J., Slomp, C. P., Stadmark, J., and Voss, M.: Efficiency of the coastal filter: Nitrogen and phosphorus removal in the Baltic Sea, *Limnology and Oceanography*, 62, S222–S238, <https://doi.org/10.1002/lno.10644>, 2017.

Börgel, F., Neumann, T., Rooze, J., Radtke, H., Barghorn, L., and Meier, H. E. M.: Deoxygenation of the Baltic Sea during the last millennium, *Frontiers in Marine Science*, 10, <https://doi.org/10.3389/fmars.2023.1174039>, 2023.

Carstensen, J., Andersen, J. H., Gustafsson, B. G., and Conley, D. J.: Deoxygenation of the Baltic Sea during the last century, *Proceedings of the National Academy of Sciences*, 111, 5628–5633, <https://doi.org/10.1073/pnas.1323156111>, 2014.

570 Conley, D. J., Carstensen, J., Aigars, J., Axe, P., Bonsdorff, E., Eremina, T., Haahti, B.-M., Humborg, C., Jonsson, P., Kotta, J., Lännergren, C., Larsson, U., Maximov, A., Medina, M. R., Lysiak-Pastuszak, E., Remeikaitė-Nikienė, N., Walve, J., Wilhelms, S., and Zillén, L.: Hypoxia Is Increasing in the Coastal Zone of the Baltic Sea, *Environ. Sci. Technol.*, 45, 6777–6783, <https://doi.org/10.1021/es201212r>, 2011.

Diaz, R. J. and Rosenberg, R.: Spreading Dead Zones and Consequences for Marine Ecosystems, *Science*, 321, 926–929, <https://doi.org/10.1126/science.1156401>, 2008.

575 Edman, M., Eilola, K., Almroth-Rosell, E., Meier, H. E. M., Wahlström, I., and Arneborg, L.: Nutrient Retention in the Swedish Coastal Zone, *Frontiers in Marine Science*, 5, <https://doi.org/10.3389/fmars.2018.00415>, 2018.

Eilola, K., Gustafson, B. G., Kuznetsov, I., Meier, H. E. M., Neumann, T., and Savchuk, O. P.: Comparison of observed and simulated dynamics of biogeochemical cycles in the Baltic Sea during 1970–2005 using three state-of-the-art numerical models, *Journal of Marine Systems*, 88, 267–284, <https://doi.org/10.1016/j.jmarsys.2011.05.004>, 2011.

580 Fennel, K. and Testa, J. M.: Biogeochemical Controls on Coastal Hypoxia, *Annual Review of Marine Science*, 11, 105–130, <https://doi.org/10.1146/annurev-marine-010318-095138>, 2019.

Fredriksson, J. P., Attard, K., Stranne, C., Koszalka, I. M., Glud, R. N., Andersen, T. J., Humborg, C., and Brüchert, V.: Hidden seafloor hypoxia in coastal waters, *Limnology and Oceanography*, 69, 2489–2502, <https://doi.org/10.1002/lno.12607>, 2024.

585 Friedland, R., Schernewski, G., Gräwe, U., Greipsland, I., Palazzo, D., and Pastuszak, M.: Managing Eutrophication in the Szczecin (Oder) Lagoon-Development, Present State and Future Perspectives, *Frontiers in Marine Science*, 5, <https://doi.org/10.3389/fmars.2018.00521>, 2019.

Geyer, B. and Rockel, B.: coastDat-2 COSMO-CLM Atmospheric Reconstruction [data set], [https://doi.org/10.1594/WDCC/coastDat-2\\_COSMO-CLM](https://doi.org/10.1594/WDCC/coastDat-2_COSMO-CLM), 2013.

590 Grelowski, A., Pastuszak, M., Sitek, S., and Witek, Z.: Budget calculations of nitrogen, phosphorus and BOD5 passing through the Oder estuary, *Journal of Marine Systems*, 25, 221–237, [https://doi.org/10.1016/S0924-7963\(00\)00017-8](https://doi.org/10.1016/S0924-7963(00)00017-8), 2000.

Griffies, S. M.: *Fundamentals of Ocean Climate Models*, Princeton University Press, Princeton, NJ, ISBN 9780691118925, 2004.

HELCOM: Sources and pathways of nutrients to the Baltic Sea., <https://helcom.fi/wp-content/uploads/2019/08/BSEP153.pdf>, (last access 2025-10-09), 2018.

595 HELCOM: HELCOM Baltic Sea Action Plan - 2021 update, <https://helcom.fi/wp-content/uploads/2021/10/Baltic-Sea-Action-Plan-2021-update.pdf>, (last access: 2025-10-09), 2021a.

HELCOM: Eutrophication - Thematic assessment 2016–2021, Baltic Sea Environment Proceedings 192, <https://helcom.fi/wp-content/uploads/2023/06/HELCOM-Thematic-assessment-of-eutrophication-2016-2021.pdf>, (last access: 2025-10-09), 2021b.

600 Jakobsen, H. H. and Markager, S.: Carbon-to-chlorophyll ratio for phytoplankton in temperate coastal waters: Seasonal patterns and relationship to nutrients, *Limnology and Oceanography*, 61, 1853–1868, <https://doi.org/10.1002/lno.10338>, 2016.

Kabel, K., Moros, M., Porsche, C., Neumann, T., Adolphi, F., Andersen, T. J., Siegel, H., Gerth, M., Leipe, T., Jansen, E., and Sinninghe Damsté, J. S.: Impact of climate change on the Baltic Sea ecosystem over the past 1,000 years, *Nature Climate Change*, 2, 871–874, <https://doi.org/10.1038/nclimate1595>, 2012.

605 Kärnä, T., Ljungemyr, P., Falahat, S., Ringgaard, I., Axell, L., Korabel, V., Murawski, J., Maljutenko, I., Lindenthal, A., Jandt-Scheelke, S., Verjovkina, S., Lorkowski, I., Lagemaa, P., She, J., Tuomi, L., Nord, A., and Huess, V.: Nemo-Nordic 2.0: operational marine forecast model for the Baltic Sea, *Geoscientific Model Development*, 14, 5731–5749, <https://doi.org/10.5194/gmd-14-5731-2021>, 2021.

610 Kuliński, K., Rehder, G., Asmala, E., Bartosova, A., Carstensen, J., Gustafsson, B., Hall, P. O. J., Humborg, C., Jilbert, T., Jürgens, K., Meier, H. E. M., Müller-Karulis, B., Naumann, M., Olesen, J. E., Savchuk, O., Schramm, A., Slomp, C. P., Sofiev, M., Sobek, A., Szymczycha, B., and Undeman, E.: Biogeochemical functioning of the Baltic Sea, *Earth System Dynamics*, 13, 633–685, <https://doi.org/10.5194/esd-13-633-2022>, 2022.

Lampe, R.: The Odra Estuary as a Filter and Transformation Area, *Acta hydrochimica et hydrobiologica*, 27, 292–297, [https://doi.org/10.1002/\(SICI\)1521-401X\(199911\)27:5<292::AID-AHEH292>3.0.CO;2-Z](https://doi.org/10.1002/(SICI)1521-401X(199911)27:5<292::AID-AHEH292>3.0.CO;2-Z), 1999.

Leibniz Institute for Baltic Sea Research: ERGOM: Ecological ReGional Ocean Model, <https://ergom.net/>, last access: 10 March 2022, 2015.

615 Mohrholz, V. and Lass, H. U.: Transports between Oderhaff and Pomeranian bight – a simple barotropic box model, *Deutsche Hydrografische Zeitschrift*, 50, 371–383, <https://doi.org/10.1007/BF02764231>, 1999.

Monsen, N. E., Cloern, J. E., Lucas, L. V., and Monismith, S. G.: A comment on the use of flushing time, residence time, and age as transport time scales, *Limnology and Oceanography*, 47, 1545–1553, <https://doi.org/10.4319/lo.2002.47.5.1545>, 2002.

Müller-Karulis, B. and Aigars, J.: Modeling the long-term dynamics of nutrients and phytoplankton in the Gulf of Riga, *Journal of Marine Systems*, 87, 161–176, <https://doi.org/10.1016/j.jmarsys.2011.03.006>, 2011.

620 Neumann, T. and Schernewski, G.: Eutrophication in the Baltic Sea and shifts in nitrogen fixation analyzed with a 3D ecosystem model, *Journal of Marine Systems*, 74, 592–602, <https://doi.org/10.1016/j.jmarsys.2008.05.003>, 2008.

Neumann, T., Siegel, H., and Gerth, M.: A new radiation model for Baltic Sea ecosystem modelling, *Journal of Marine Systems*, 152, 83–91, <https://doi.org/10.1016/j.jmarsys.2015.08.001>, 2015.

625 Neumann, T., Koponen, S., Attila, J., Brockmann, C., Kallio, K., Kervinen, M., Mazeran, C., Müller, D., Philipson, P., Thulin, S., Väkevä, S., and Ylöstalo, P.: Optical model for the Baltic Sea with an explicit CDOM state variable: a case study with Model ERGOM (version 1.2), *Geoscientific Model Development*, 14, 5049–5062, <https://doi.org/10.5194/gmd-14-5049-2021>, 2021.

Neumann, T., Radtke, H., Cahill, B., Schmidt, M., and Rehder, G.: Non-Redfieldian carbon model for the Baltic Sea (ERGOM version 1.2) – implementation and budget estimates, *Geoscientific Model Development*, 15, 8473–8540, <https://doi.org/10.5194/gmd-15-8473-2022>, 2022.

630 Neumann, T., Schernewski, G., and Friedland, R.: Model code and output for "Transformation Processes in the Oder Lagoon as seen from a Model Perspective" paper [code], <https://doi.org/10.5281/zenodo.14236528>, last access: 28 November 2024, 2024.

Pastuszak, M., Witek, Z., Nagel, K., Wielgat, M., and Grelowski, A.: Role of the Oder estuary (southern Baltic) in transformation of the riverine nutrient loads, *Journal of Marine Systems*, 57, 30–54, [https://doi.org/https://doi.org/10.1016/j.jmarsys.2005.04.005](https://doi.org/10.1016/j.jmarsys.2005.04.005), 2005.

Piehl, S., Friedland, R., Heyden, B., Leujak, W., Neumann, T., and Schernewski, G.: Modeling of Water Quality Indicators in the Western Baltic Sea: Seasonal Oxygen Deficiency, *Environmental Modeling & Assessment*, 28, 429–446, <https://doi.org/10.1007/s10666-022-09866-x>, 2023.

635 Radtke, H., Lipka, M., Bunke, D., Morys, C., Woelfel, J., Cahill, B., Böttcher, M. E., Forster, S., Leipe, T., Rehder, G., and Neumann, T.: Ecological ReGional Ocean Model with vertically resolved sediments (ERGOM SED 1.0): coupling benthic and pelagic biogeochemistry of the south-western Baltic Sea, *Geoscientific Model Development*, 12, 275–320, <https://doi.org/10.5194/gmd-12-275-2019>, 2019.

640 Rutgersson, A., Kjellström, E., Haapala, J., Stendel, M., Danilovich, I., Drews, M., Jylhä, K., Kujala, P., Larsén, X. G., Halsnæs, K., Lehtonen, I., Luomaranta, A., Nilsson, E., Olsson, T., Särkkä, J., Tuomi, L., and Wasmund, N.: Natural hazards and extreme events in the Baltic Sea region, *Earth System Dynamics*, 13, 251–301, <https://doi.org/10.5194/esd-13-251-2022>, 2022.

645 Ruvalcaba Baroni, I., Almroth-Rosell, E., Axell, L., Fredriksson, S. T., Hieronymus, J., Hieronymus, M., Brunnabend, S.-E., Gröger, M., Kuznetsov, I., Fransner, F., Hordoir, R., Falahat, S., and Arneborg, L.: Validation of the coupled physical–biogeochemical ocean model NEMO–SCobi for the North Sea–Baltic Sea system, *Biogeosciences*, 21, 2087–2132, <https://doi.org/10.5194/bg-21-2087-2024>, 2024.

Schernewski, G., Friedland, R., Carstens, M., Hirt, U., Leujak, W., Nausch, G., Neumann, T., Petenati, T., Sagert, S., Wasmund, N., and von Weber, M.: Implementation of European marine policy: New water quality targets for German Baltic waters, *Marine Policy*, 51, 305–321, <https://doi.org/10.1016/j.marpol.2014.09.002>, 2015.

650 Schernewski, G., Jekat, M., Kösters, F., Neumann, T., Steffen, S., and von Thenen, M.: Ecosystem Services Supporting Environmental Impact Assessments (EIAs): Assessments of Navigation Waterways Deepening Based on Data, Experts, and a 3D Ecosystem Model, *Land*, 13, <https://doi.org/10.3390/land13101653>, 2024.

Schernewski, G., Neumann, T., Piehl, S., and Swer, N. M.: Ecosystem-Model-Based Valuation of Ecosystem Services in a Baltic Lagoon: Long-Term Human Technical Interventions and Short-Term Variability, *Environments*, 12, <https://doi.org/10.3390/environments12020035>, 2025a.

655 Schernewski, G., Neumann, T., Piehl, S., and von Weber, M.: New approaches to unveil the unknown: oxygen depletion and internal eutrophication in a Baltic lagoon over decades, *Frontiers in Environmental Science*, Volume 13 - 2025, <https://doi.org/10.3389/fenvs.2025.1620191>, 2025b.

Sieifert, T., Tauber, F., and Kayser, B.: Digital topography of the Baltic Sea [data set], <https://www.io-warnemuende.de/topography-of-the-baltic-sea.html>, last access: 27 July 2020, 2008.

660 Vahtera, E., Conley, D. J., Gustafsson, B. G., Kuosa, H., Pitkänen, H., Savchuk, O. P., Tamminen, T., Viitasalo, M., Voss, M., Wasmund, N., and Wulff, F.: Internal ecosystem feedbacks enhance nitrogen-fixing cyanobacteria blooms and complicate management in the Baltic Sea, *Ambio*, 36, 186–194, 2007.

Vollenweider, R. A.: Advances in defining critical loading levels for phosphorus in lake eutrophication., <https://api.semanticscholar.org/CorpusID:131391058>, (last access: 2025-10-09), 1976.

665 Vybernaite-Lubiene, I., Zilius, M., Bartoli, M., Petkuviene, J., Zemlys, P., Magri, M., and Giordani, G.: Biogeochemical Budgets of Nutrients and Metabolism in the Curonian Lagoon (South East Baltic Sea): Spatial and Temporal Variations, *Water*, 14, <https://doi.org/10.3390/w14020164>, 2022.

Winton, M.: A Reformulated Three-Layer Sea Ice Model, *Journal of Atmospheric and Oceanic Technology*, 17, 525–531, [https://doi.org/10.1175/1520-0426\(2000\)017<0525:ARTLSI>2.0.CO;2](https://doi.org/10.1175/1520-0426(2000)017<0525:ARTLSI>2.0.CO;2), 2000.